Electronic Journal of Structural Engineering

Original Article

Cite this: DOI:10.56748/ejse.234083

Received Date: 4 January 2023
Accepted Date: 28 June 2023

1443-9255
https://ejsei.com/ejse

Numerical Study on the Various Profile Sections of Concrete Filled Steel Tubular Columns Under Compression

Vinay Kumar Singh [a]*, Pramod Kumar Gupta [b], & S M Ali Jawaid [a]
[a] Department of Civil Engineering, Madan Mohan Malviya University of Technology, Gorakhpur, Uttar Pradesh, India
[b] Department of Civil Engineering, Indian Institute of Technology Roorkee, India
*Corresponding Author: vinay011990@gmail.com

Abstract

Axial load carrying capacity for wide range of short concrete filled steel tubular (CFST) members with different cross-sectional profiles has been evaluated in the presented manuscript. Numerical studies are carried out through Finite-Element based demonstration and it has been accomplished in ABAQUS 6.13 package for relevancy of analytically predicted axial load carrying capacity by Unified Formula. To validate the results from the Unified Formula with the experimentally available literature, finite element-based models have been generated for hollow and solid sections of CFST columns. These sections are circular, octagonal, and square in profiles. A total of 31 hollow and 24 solid circular columns, 9 hollow and 9 solid octagonal columns and in last 9 hollow and 38 solid square CFST columns are examined for the persistence of the results. Obtained results through simulated models has been evaluated and validated with the existing results of different researchers. Through close inspection it is found that the proposed Unified formula predicts satisfactory results when compared with the result of established models. Further it is concluded that displacement in the direction of applied load is not uniform throughout the length of CFST columns. Therefore, using ring confinement technique for those regions, applied forces may be distributed more uniformly throughout the length of the members.

Keywords

ABAQUS, Axial Load, Concrete filled steel tube (CFST), Numerical Analysis, Ring confinement, Unified formula

1. Introduction

Concrete filled Steel tubes are gaining intensified usage in distinct field of construction throughout the world, especially in Far East and South-East Asian countries. Some benefits of this from structural perspective is such as confinement caused by the steel tube, which will enhance the strength and stiffness of CFST columns. Additionally, it makes both regular and high strength concrete more ductile. Economic benefits include quicker construction with less labor-intensive formwork, less expensive painting and fireproofing due to the smaller open section size compared to other sections. While other cross-sections of CFST are primarily employed for architectural and functional purposes, several cross-sections of CFST columns are taken into consideration, including square, round, and rectangular ones. To further improve the confinement of concrete and minimize column size, reinforcement can be substituted with solid sections in addition to being used to promote ductility and fire resistance.

The prime objective of the presented document is to investigate a unified formula for axial compressive strength of concrete filled steel tubular columns which include experimental and analytical studies. The numerical method is used in this manuscript to verify the axial compressive strength determined by the unified formula. Further it has been verified by the CAE-based ABAQUS 6.13 software. The modeling and analysis of CFST columns are very thoroughly provided by this finite element-based tool, which also aids in understanding the behavior and failure mechanisms of axially loaded CFST columns with diversified geometric configurations, various parameters, and applied loads.

2. Past Research

Experimental approach to analyze CFST column have been going on from decades for improvement of CFST as structural member. To examine a model or to verify the outcomes of expected design methodologies, fundamental information from experimental results is effective. The precise failure mechanism and behavior of the CFST column under various conditions are predicted by the experimental technique, which aids in the creation of design requirements.

An assessment for experimental studies and substantial investigation had been steered by Shanmugam and Lakshmi (2001) on CFST columns. Their manuscript described some of the research work accentuated by them as well as it includes the work accomplished by distinct scholars in the same area up to year 1999.

In recent years, the usage of high strength concrete in CFST column has been growing constantly whereas, for self-compacting and high-performance concrete, which is highly flowable concrete, is also suitable for CFST due to no requirement of formwork and mechanical vibration. This type of concrete provides significant advantages over normal concrete and makes construction more economic in less time. Yu Q. et al. (2008) performs several tests over CFST column by using these types of concrete and applying eccentric load. Which results failure of circular column is shearing mode while square stub buckle outwards. Compressive resistance of column increases by increasing the strength of infilled concrete.

Behavior of CFST stub columns with square, circular, and rectangular section under eccentric partial compression is investigated by Yang et al. (2011) with eccentricity ratio from 0 to 0.4 and it is found that as the load eccentricity ratio increases load resistance of column decreases. The capacity index of partially loaded circular CFST stud column is more than that of rectangular and square CFST column.

A good number of experiments had been performed by Han et al. (1997) and compare those results with various available code. He found that methodology intended by AISC-LRFD (2000), AIJ (2008), EC4 (2005) and DL/T 5085 (1999) codal provisions predicts the conservative compressive strength for CFST column than the normal strength of the columns. These provisions can't be used for long or slender columns as it didn't provide the satisfactory results. It was found that using lower strength concrete about 30 MPa, ductility of circular CFST columns is higher than the heigh strength concrete about 60 MPa. This prevails upto d/t ratio of 80 as suggested by Lee et al. (2011).

Concrete filled steel sections are found to be more ductile than steel hollow sections. Ductility of square, rectangular, hexagonal, and circular sections was specified as 4, 3.1, 11.6, 19.8 respectively. So, it is obvious that the circular section takes greater ductility than any other sections which was tested by Evirgen et al. (2014).

High strength and low weight members take ample significance in seismic design of structures because seismic response diminished due to lesser mass of structure. Xiong M. X. et al. (2017) performs a significant number of experiments on high and ultra-high strength material which shows that using ultra high strength concrete (UHSC) and high compressive resistance required in high rise building can be attained without difficulty and the essential strength can be increased further by using high tensile steel (HTS).

High grade concrete has adverse effect on the ductility of the circular CFST column Lee et al. (2011) upto a diameter to thickness (d/t) ratio of 80. Ductility of CFST with lower grade (30 MPa) concrete is higher than the ductility with higher grade (60 MPa) concrete. The circular CFST column performs well under eccentric loading according to KBCS and AISC, although Eurocode 4 overestimates it. Henceforth, for large diameter to thickness ratio more research is required for circular CFST columns with high strength materials as suggested by Lee et al. (2011).

2.1 Unified Formula of Yu M. et. al. (2010)

A unified formulation for both hollow and solid CFST columns is given by Yu M. et al. (2010) in his manuscript and is based on the theory of elasticity and regression analysis of test data. The suggested approach strives to offer more precise and effective design alternatives for CFST columns. He utilizes the analytical solution of the elastic deformation of the column under axial compression to construct formulas that yield composite compressive strength. The compressive strength's analytical form is then calibrated by adding several correlation coefficients that were discovered through the regression analysis of test data. The research also constructs a unified stability factor formula for both solid and hollow CCFST long columns under axial compression based on the Perry model. Further investigation revealed that while solid concrete-filled steel tube components had undergone significant experimental and theoretical examination, the study of hollow concrete-filled steel tube (H-CFST) was insufficient and clearly needed. A design that just uses the S-CFST for H-CFST formula is frequently overly conservative. From the perspective of mathematical modeling and material property continuity, H-CFST and S-CFST components can be created by adhering to a single formula. The model considers the combined action of the concrete and steel in CCFST columns. The model is based on the elasticity theory and assumes that the concrete core and steel tube both respond elastically to axial compression. The equilibrium equation of the composite column and the stress-strain relationship between the steel tube and concrete core are used in the model to determine the compressive strength of CCFST columns. According to his research, numerous variables, including the cross-sectional area of the steel tube, the thickness of the concrete core, and the characteristics of the steel and concrete materials, have an impact on the compressive strength of CCFST columns. The calculation considers the effects of various variables, including the elastic modulus of the steel and concrete materials, the concrete material's Poisson's ratio, and the column's slenderness ratio. Both solid and hollow CCFST long columns can use the formula. The results of the tests demonstrate how well the suggested formulas predict the compressive strength and stability factor of CCFST columns during axial compression.

To predict the axial strength, the elastic deformation of a circular CFST is divided into a uniaxial compression and a plane strain problem. The solution of thick-walled cylinder and displacement compatibility is used to predict the formula of axial strength. And it is applicable for both hollow and solid circular sections. For engineering practices, commonly used steel grade is of the range between 235 to 420 MPa and concrete grade is of 30 to 80 MPa. So, for solid steel ratio lie between 0.04 to 0.2 unified formula for strength and axial load resisting capacity of a circular CFST column which is given as:

$$f_{sc} = \frac{1+(1+0.5\Omega)\xi}{1+\alpha} f_{ck} \quad (1)$$

$$Q_o = f_{sc}A_{sc} = \left(1 + 0.5\frac{\xi}{1+\xi}\Omega\right)\left(f_{ck}A_c + f_yA_s\right) \quad (2)$$

Where, coefficient of confinement is ξ, solid concrete ratio is Ω (for solid CFST column Ω =1) and steel ratio is α. f_{ck}, f_y is the characteristic strength of concrete and steel respectively and A_c, A_s is the cross-sectional area of concrete and steel respectively. By Eq. (2) polygon section is assumed as a special case of circular section in which polygon section is transformed into an equivalent circular section. After that the solution is modified by using the correction factor. Regular polygonal section is demarcated into an effective enhanced and non-enhanced zone. The enhanced zone then approaches that of a circular section. The unified combined strength and axial load bearing capacity of a general polygonal CFST column is given as:

$$f_{sc} = \frac{1+(1+0.5\lambda_e)\xi}{1+\alpha} f_{ck} \quad (3)$$

$$Q_{po} = f_{sc}A_{sc} = \left(1 + 0.5\frac{\xi}{1+\xi}\lambda_e\right)\left(f_{ck}A_c + f_yA_s\right) \quad (4)$$

Where, λ_e is confinement effectiveness coefficient ($\lambda_e = \lambda_h\lambda_n$), λ_h is the hollow confinement effectiveness coefficient ($\lambda_h = \Omega$), λ_n is the polygon confinement effectiveness coefficient which is given as:

$$\lambda_n = \frac{n^2-4}{n^2+20} \quad (5)$$

n is the number of sides of polygon column. This unified formula can be used for solid and hollow sections of CFST columns. For a solid circular CFST column, $\lambda_h = \lambda_n = 1$.

In the past, a few years back sufficient research had been performed by intellectuals and diverse formulas were proposed by them for axial load carrying capacity of CFST columns. These members have distinct geometry and different cross-sectional areas. Yu M. et al. (2010) proposed a unified formula for various sectional profiles of CFST column to calculate axial load capacity. Which are also relevant for short and slender columns.

Numerous computational models were purported by various scholars to estimate the axial compression strength of stub column like Dey P. et al. (2019), Dai X. H. et al. (2014) Thai, H. T. (2014) and many more. The finite element approach was also embraced by these researchers for exploration of CFST columns. In this paper a finite element program called ABAQUS 6.13 is used for the stimulation of short CFST columns of different sections profile as proposed by different researchers.

Primarily, plentiful experimental, analytical, and numerical research work are yet to be carried out to establish the actual comportment of CFST column for constraints likes effect of slenderness ratio, different section, lateral cyclic loading, ductility, long term effect (creep and shrinkage), second order effect, residual stress, stiffeners, and effect of increase in temperature on the failure mode and compressive strength of CFST column. Additional experimental work is also obligatory to investigate the behavior of CFST due to presence of fly ash or any other fiber in concrete infill. This exploration could determine the thickness of used steel tube. Particularly for confinement and behavior of hollow and octagonal shaped CFST columns depends on the thickness of used steel tube. Most recently a few other techniques are also used like introducing ring at regular intervals to enhance the confinement, introducing corrugation in steel to avoid direct axial stress in steel. Abundant practices are accessible on which further experimentations are obligatory to be done. This required to explore the behavior of CFST column with diverse loading condition with few restrictions like long term effect and techniques which looked-for to enhance the confinement of concrete. The behavior of slender columns, asymmetrical CFST columns and behavior of compressed infilled concrete in CFST, all could be analyzed by using a single Unified formula which is applicable for all section types.

3. Description of Numerical Model

In the presented paper, Abaqus 3D models of diverse section profiles (Circular, Rectangular, Square, Octagonal) for solid and hollow short CFST columns were stimulated for study.

3.1 Modelling of steel tube

The modelled part of steel was assigned property using "Plastic" option. For analysis, the Youngs modulus of steel (E_s) was an average value taken as 200,000 N/mm^2 as mentioned. For each samples Poisson's ratio (μ_s) was taken as per the literature if it provided, else it is taken as 0.29. Ultimate stress (f_u) was taken as per Zhong Tao et al. (2013) unless it is specifically mentioned in the literature.

3.2 Modelling of concrete

To describe the behavior of confined concrete of CFST columns it was modelled as continuum, plasticity-based and damaged to represent the plastic behavior of concrete. Concrete was modelled as a solid and extruded as per the literature. The modelled part was assigned the concrete damaged plasticity (CDP) to every samples. The young's modulus for concrete (E_c) was considered as 5000√ (f_{ck}) unless not mentioned in literatures, dilation angel (k) was taken as 30 if not mentioned, Poisson ratio of concrete (μ_c) was considered between 0.2 to 0.1 (Poisson ratio decrease as the characteristic strength of concrete increase). CDP property for concrete was calculated as per recommended by Hafezolghorani, M. et al (2017), the ratio of biaxial to the uniaxial compressive yield stress (f_{b0}/f_{c0}) is considered as 1.16, the ratio K of the second stress invariant on the tensile meridian to that on the compressive meridian for the yield function is considered as 0.667 and viscosity coefficient was taken as 0.001. The compressive stress and elastic strain along with tensile stress and inelastic strain was calculated as recommended by Hafezolghorani, M et al. (2017). Same parameters were assigned for the hollow concrete section which was modelled by cut extruding of solid concrete section. Every model was partitioned symmetrically using datum plan offset from principal axis as shown below in Fig. 1 which depicts a typical model of steel tube, solid concrete, and hollow concrete section of different cross-section profiles.

3.3 Seeding, element type and mesh

Global seeding is used when seeding is same at all regions of the model otherwise seeding by edge is used. In this paper edge seeding has been done to both the part instances (plain concrete or steel tube) of modelled CFST column.

As per the available literature by Dai, X. H. et al. (2014) and Dey, P. et al. (2019) we adopted only C3D8R in the presented manuscript because it is most suitable for the solid and hollow plain concrete. Unlikely other types of elements set, it converges quickly because it does not require fine or small size mess which saves time of stimulation for large number of samples. The steel tube of columns was modelled using S4R (4-node reduced integration shell elements). It has 6 DOF per node and provides an

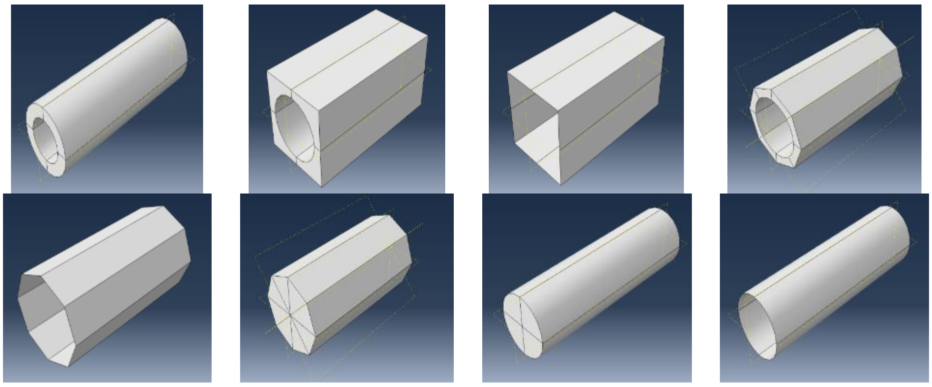

Fig. 1. Typical model of steel tube, solid & hollow concrete section of different cross-section.

accurate solution to most shell type models. Based on the available literature Thai, H. T et al. (2014), for the steel tube and plain concrete of hollow or solid CFST column, the smallest and largest element sizes are chosen as D/23 and D/13, respectively, where D is the width and diameter of the different sections profile.

3.4 Interaction of CFST column

To make steel tube and concrete solid behave as a single unit as a composite structure there should be surface to surface interaction between both instances. For surface-to-surface interaction Tie constraint was used for which hard concrete outer surface which is confined by steel tube was used as master surface and the inner surface of steel tube was used as a slave surface.

3.5 Boundary condition

In the proposed model of the CFST column the bottom of the steel tube displacement and rotation in all direction is restricted ($\Delta_x = \Delta_y = \Delta_z = 0$ & $\theta_x = \theta_y = \theta_z = 0$) that is fixed support. For the concrete bottom, BC is pinned support that is displacement in all direction is restricted ($\Delta_x = \Delta_y = \Delta_z = 0$). For the top surface of concrete, displacement in lateral direction was restricted but allowed in downward direction ($\Delta_x = \Delta_y = 0$). For the steel top surface displacement in lateral direction was suspended but allowed in the downward direction equal to the displacement allowed for the concrete top surface. Rotation of the steel top surface was also restricted ($\Delta_x = \Delta_y = 0$ & $\theta_x = \theta_y = \theta_z = 0$). Two sections were created and assigned one is for concrete that is solid, homogenous, and the other one is shell, homogenous for steel tubes.

4. Verification of Finite Element Models

The developed model of CFST column having cross section of circular, square, rectangular & hexagonal is proven through previously carried out experimental research work on different profile sections of CFST columns. All the experimental data of axial load bearing capacity of 31 no. of hollow circular Zhong, S.T. et al.(2003), 24 no. of solid circular Li B. et al. (2005) & Han L. H. et al. (1997), 9 no. of hollow octagonal Zhong S. T. et al. (2006), 9 no. of solid octagonal Zha X. X. et al. (2010), 38 no. of solid square Liu D. L. et al. (2005), Schneider S. P. (2005), Zhang S. M. et al. (1998) & Liu D. L. et al. (2005) and 9 no. of hollow square Zhong S. T. et al. (2006) short CFST columns specimens were collected and the calculated axial load bearing capacity of these CFST columns using the unified formula as proposed by Yu M. et al. (2010) from literatures Yu M. et al. (2013) and Yu M. et al. (2010) is obtained. Tables 1 and 2 summarized the validation of hollow and solid circular CFST columns respectively, Tables 3 and 4 present the validation of hollow and solid octagonal CFST columns respectively and Tables 5 and 6 used to validate the hollow and solid square CFST columns respectively as shown below. Where, 'D' is the overall diameter of a circular or octagonal section, 'B' is the sides of a square or octagonal section. 'H' is the overall height or length of a CFST column, T_S and T_C is the steel thickness and thickness of concrete respectively. Characteristic strength of the concrete and yield strength of steel is presented by f_{ck} and f_y respectively. The axial load capacity of CFST column obtained by analytically as per the formula derived by Yu M. et al. (2010), experimentally obtained from previous literatures, and numerically as per proposed FE models is symbolized by N_{CAL}, N_{EXP}, and N_O respectively.

Table 1. Comparison of Formula based, Experimental Based, and FE models-based results for hollow circular CFST column.

Ref. No.	Ser. No.	Name	(D) mm	(T_S) mm	(T_C) mm	(H) mm	(fy) MPa	(fck) MPa	N_{CAL} kN	N_{EXP} kN	N_O kN	N_O /N_{CAL}	N_O /N_{EXP}
	1	A-1	296	2.0	54.0	900	196.0	32.0	1834	2058	1844.000	1.005	0.896
	2	A-2	296	2.0	54.0	900	196.0	32.0	1834	2058	1844.000	1.005	0.896
	3	A-3	296	2.0	57.0	900	196.0	32.0	1889	2136	2017.156	1.068	0.944
	4	A-4	296	3.0	49.0	900	228.6	32.0	2131	2205	209.975	0.099	0.095
	5	A-7	296	4.0	54.0	900	171.5	32.0	2211	2568	2340.796	1.059	0.912
	6	A-8	296	4.0	57.0	900	171.5	32.0	2265	2450	2408.675	1.063	0.983
	7	A-9	296	4.0	60.0	900	171.5	32.0	2316	2568	2455.030	1.060	0.956
	8	A1-1	296	2.0	63.0	900	196.0	34.1	2088	2391	2412.998	1.156	1.009
	9	A1-2	296	2.0	68.0	900	196.0	34.1	2174	2450	2518.189	1.158	1.028
	10	A1-3	296	2.0	73.0	900	196.0	34.1	2255	2587	2615.938	1.160	1.011
	11	A1-4	296	3.0	66.0	900	228.6	34.1	2528	2450	2416.180	0.956	0.986
	12	A1-5	296	3.0	71.0	900	228.6	34.1	2611	2646	2649.061	1.015	1.001
	13	A1-6	296	3.0	66.0	900	171.5	34.1	2293	2666	2559.650	1.116	0.960
Zhong S.T. et al. (2003)	14	A1-7	296	4.0	66.0	900	171.5	34.1	2511	2840	2714.133	1.081	0.956
	15	A1-8	296	4.0	66.0	900	171.5	34.1	2511	2842	2714.133	1.081	0.955
	16	A1-9	296	4.0	65.0	900	171.5	34.1	2494	2960	2690.983	1.079	0.909
	17	H3-a	165	4.8	57.9	500	248.7	26.4	1361	1363	1316.701	0.967	0.966
	18	H3-b	165	4.8	57.9	500	248.7	26.4	1361	1461	1316.701	0.967	0.901
	19	H3-c	165	4.8	53.4	500	248.7	26.4	1344	1336	1286.093	0.957	0.963
	20	H3-d	165	4.8	53.4	500	248.7	26.4	1344	1334	1286.093	0.957	0.964
	21	H3-e	165	4.8	40.4	500	248.7	26.4	1276	1187	1161.385	0.910	0.978
	22	H3-f	165	4.8	40.4	500	248.7	26.4	1276	1177	1161.385	0.910	0.987
	23	YL-1	200	2.9	22.7	600	300.0	57.5	1507	1570	1514.918	1.005	0.965
	24	YL-2	200	2.9	20.5	600	300.0	57.5	1446	1480	1358.174	0.939	0.918
	25	YL-3	200	2.9	20.5	600	300.0	57.5	1446	1530	1358.174	0.939	0.888
	26	YL-4	200	2.9	26.4	600	300.0	57.5	1604	1740	1546.116	0.964	0.889
	27	YL-5	200	2.9	22.7	600	300.0	57.5	1507	1500	1514.918	1.005	1.010
	28	YL-6	200	2.9	26.4	600	300.0	57.5	1604	1690	1546.116	0.964	0.915
	29	YL-7	200	4.7	24.0	600	240.0	57.5	1752	1695	1675.126	0.956	0.988
	30	YL-8	200	4.7	23.2	600	240.0	57.5	1732	1580	1595.356	0.921	1.010
	31	YL-9	200	4.6	26.3	600	240.0	57.5	1791	1778	1798.985	1.004	1.012

Table 2. Comparison of formula based, experimental based, and F E models-based results for solid circular CFST columns.

Ref. No.	Ser. No.	Name	(D) mm	(T_S) mm	(T_C) mm	(H) mm	(fy) MPa	(fck) MPa	N_{CAL} kN	N_{EXP} kN	N_O kN	N_O /N_{CAL}	N_O /N_{EXP}
Li B. and Hao R. X. (2005)	1	SC-1	164	3.8	78.2	520	342	30.5	1564	1650	1664.578	1.064	1.009
	2	SC-2	164	3.8	78.2	520	342	30.5	1564	1710	1664.578	1.064	0.973
	3	SC-3	164	3.8	78.2	520	342	30.5	1564	1600	1664.578	1.064	1.040
	4	SC-4	159	4.8	74.7	520	366	30.5	1806	1600	1769.191	0.980	1.106
	5	SC-5	159	4.8	74.7	520	366	30.5	1806	1700	1769.191	0.980	1.041
	6	SC-6	159	4.8	74.7	520	366	30.5	1806	1600	1769.191	0.980	1.106
	7	SC-7	159	5.2	74.3	520	379	30.5	1951	1800	1874.409	0.961	1.041
	8	SC-8	159	5.2	74.3	520	379	30.5	1951	1850	1874.409	0.961	1.013
	9	SC-9	159	5.2	74.3	520	379	30.5	1951	1700	1874.409	0.961	1.103
	10	SC-10	159	6.3	73.2	520	360	30.5	2136	2000	1994.051	0.934	0.997
	11	SC-11	159	6.3	73.2	520	360	30.5	2136	1950	1994.051	0.934	1.023
	12	SC-12	159	6.3	73.2	520	360	30.5	2136	2100	1994.051	0.934	0.950
Han L. H. (1997)	13	SCCS3-2	178.0	9.0	80.0	360	283.0	36.7	2751	2671	3078.043	1.119	1.152
	14	SCCS4-2	179.0	5.5	84.0	360	266.0	36.6	1922	2034	2059.158	1.071	1.012
	15	SCCS5-2	174.0	3.0	84.0	360	266.0	34.6	1408	1642	1553.001	1.103	0.946
	16	SCCS6-3	159.8	6.3	73.6	476	482.5	53.4	3095	2350	2963.670	0.958	1.261
	17	SCCS7-4	115.9	4.9	53.1	350	309.5	53.4	1260	1174	1291.441	1.025	1.100
	18	SCCS8-3	141.8	4.3	66.6	420	433.0	53.4	1945	1618	1578.617	0.812	0.976
	19	SCCS9-3	141.8	3.9	67.0	337	357.7	53.4	1656	1150	1684.550	1.017	1.465
	20	SCCS10-3	165.7	5.1	77.8	494	373.3	53.4	2449	2309	1953.148	0.798	0.846
	21	SCCS11-1	133.1	4.5	62.1	397	324.3	53.4	1526	1535	1501.883	0.984	0.978
	22	SCCS12-3	113.6	3.2	53.6	337	354.6	53.4	1070	1145	1268.008	1.185	1.107
	23	SCCS13-1	111.3	2.0	53.7	339	354.6	53.4	847	894	809.147	0.955	0.905
	24	SCCS14-1	130.6	2.3	63.0	396	324.6	53.4	1116	1250	1215.341	1.089	0.972

Table 3. Comparison of formula based, experimental, and FE models-based results for hollow octagonal CFST columns.

Ref. No.	Ser. No.	Name	(B) mm	(T_S) mm	(H) mm	(r) mm	(fy) MPa	(fck) MPa	N_{CAL} kN	N_{EXP} kN	N_O kN	N_O /N_{CAL}	N_O /N_{EXP}
Zhong S.T. (2006)	1	1C-1	118.9	2.50	600	111.5	334.6	40.5	1990.0	2100	1869.755	0.940	0.890
	2	1C-2	118.9	2.50	600	111.5	334.6	40.5	1990.0	1830	1869.755	0.940	1.022
	3	2C-1	118.6	3.00	600	100.5	317.3	40.5	2407.7	2160	2239.806	0.930	1.037
	4	2C-2	118.6	3.00	600	100.1	317.3	40.5	2420.6	2250	2170.483	0.897	0.965
	5	3C-1	118.1	3.80	600	99.5	315.0	40.5	2643.1	2580	2564.644	0.970	0.994
	6	3C-2	118.1	3.80	600	99.2	315.0	40.5	2653.3	2770	2573.009	0.970	0.929
	7	5C-1	117.6	4.75	600	99.0	315.8	46.0	3090.2	2900	2833.658	0.917	0.977
	8	6C-1	117.6	4.75	600	98.8	315.8	28.4	2539.8	3200	2553.243	1.005	0.798
	9	6C-2	117.6	4.75	600	100.2	315.8	28.4	2506.9	3080	2519.563	1.005	0.818

Table 4. Comparison of formula based, experimental, and FE models-based results for solid octagonal CFST columns.

Ref. No.	Ser. No.	Name	(D) mm	(T_S) mm	(H) mm	(fy) MPa	(fck) MPa	N_{CAL} kN	N_{EXP} kN	N_O kN	N_O /N_{CAL}	N_O /N_{EXP}
Zha X. X. (2010)	1	2HN	150	2.0	300	341.3	25.5	903.5	989	1028.902	1.139	1.040
	2	3HN	150	3.2	300	300.2	25.5	1068.4	1094	1075.559	1.007	0.983
	3	4HN	150	4.0	300	294.3	25.5	1197.3	1316	1333.032	1.113	1.013
	4	2MN	150	2.0	300	341.3	18.5	781.0	771	941.8474	1.206	1.222
	5	3MN	150	3.2	300	300.2	18.5	949.8	916	1145.425	1.206	1.250
	6	4MN	150	4.0	300	294.3	18.5	1081.3	1193	1300.610	1.203	1.090
	7	2LN	150	3.2	300	341.3	14.1	703.2	856	867.4493	1.234	1.013
	8	3LN	150	4.0	300	300.2	14.1	874.6	1117	1056.942	1.208	0.946
	9	4LN	150	4.0	300	294.3	14.1	1007.8	968	1202.925	1.194	1.243

Table 5. Comparison of formula based, experimental based, and FE models-based results for hollow square CFST columns.

Ref. No.	Ser. No.	Name	(B) mm	(T_S) mm	(H) mm	(r) mm	(fy) MPa	(fck) MPa	N_{CAL} kN	N_{EXP} kN	N_O kN	N_O /N_{CAL}	N_O /N_{EXP}
Zhong S.T. (2006)	1	1D-1	238	2.50	600	93.7	334.6	40.5	1935	1700	2024.106	1.046	1.191
	2	1D-2	238	2.50	600	93.0	334.6	40.5	1952	1900	2029.265	1.040	1.068
	3	2D-1	237.4	3.00	600	81.0	317.3	40.5	2318	1990	2414.908	1.042	1.214
	4	2D-2	237.4	3.00	600	81.4	317.3	40.5	2310	2400	2406.359	1.042	1.003
	5	3D-1	237.1	3.80	600	80.0	315.0	40.5	2551	2190	2658.629	1.042	1.214
	6	5D-1	237.8	4.75	600	79.2	315.8	46.0	3036	2990	3334.119	1.098	1.115
	7	5D-2	237.8	4.75	600	79.0	315.8	46.0	3039	2420	3339.109	1.099	1.380
	8	6D-1	237.3	4.75	600	80.0	315.8	28.4	2441	2880	2678.332	1.097	0.930
	9	6D-2	120	4.75	360	79.9	315.8	28.4	2443	2400	2682.351	1.098	1.118

Table 6. Comparison of formula based, experimental based, and FE models-based results for solid square CFST column.

Ref. No.	Ser. No.	Name	(B)	(T_S)	(H)	(f_y)	(f_{ck})	N_{CAL}	N_{EXP}	N_O	N_O/N_{CAL}	N_O/N_{EXP}
			mm	mm	mm	MPa	MPa	kN	kN	kN		
Liu D. L. (2005)	1	R1-1	120.0	4.0	360.0	495.0	47.9	1673	1701	1661.144	0.993	0.977
	2	R1-2	120.0	4.0	360.0	495.0	47.9	1673	1657	1661.144	0.993	1.003
	3	R4-1	130.0	4.0	390.0	495.0	47.9	1878	2020	1849.705	0.985	0.916
	4	R4-2	130.0	4.0	390.0	495.0	70.7	2217	2018	1999.458	0.902	0.991
	5	R7-1	106.0	4.0	320.0	495.0	70.7	1622	1749	1644.617	1.014	0.940
	6	R7-2	106.0	4.0	320.0	495.0	70.7	1622	1824	1644.617	1.014	0.902
	7	R10-1	140.0	4.0	420.0	495.0	70.7	2489	2752	2572.704	1.034	0.935
	8	R10-2	140.0	4.0	420.0	495.0	70.7	2489	2828	2572.704	1.034	0.910
Liu D. L. and Gho W. M. (2005)	9	A1	120.0	5.8	360.0	300.0	66.0	1702	1697	1790.653	1.052	1.055
	10	A2	120.0	5.8	360.0	300.0	84.2	1917	1919	1961.620	1.023	1.022
	11	A3-1	200.0	5.8	600.0	300.0	66.0	3918	3996	3918.395	1.000	0.981
	12	A3-2	200.0	5.8	600.0	300.0	66.0	3918	3862	3918.395	1.000	1.015
	13	A9-1	120.0	4.0	360.0	495.0	44.3	1627	1739	1716.190	1.055	0.987
	14	A9-2	120.0	4.0	360.0	495.0	44.3	1627	1718	1716.190	1.055	0.999
	15	A12-1	130.0	4.0	390.0	495.0	44.3	1823	1963	1855.393	1.018	0.945
	16	A12-2	130.0	4.0	390.0	495.0	44.3	1823	1988	1855.393	1.018	0.933
Schneider S. P. et al. (1998)	17	S1	127.0	3.2	610.0	356.0	25.8	1024	917	965.590	0.943	1.053
	18	S2	127.0	4.3	610.0	357.0	22.0	1196	1095	1188.940	0.994	1.086
	19	S3	127.0	4.6	610.0	322.0	20.2	1117	1113	1187.275	1.063	1.067
	20	S4	127.0	5.7	610.0	312.0	20.2	1271	1202	1330.451	1.047	1.107
	21	S5	127.0	7.5	610.0	347.0	20.2	1699	2069	1822.380	1.073	0.881
Zhang S. M. et al. (2005)	22	1	142.1	3.0	426.3	255.1	43.7	1309	1360	1401.468	1.071	1.030
	23	2	142.1	3.0	426.3	255.1	43.7	1309	1400	1401.468	1.071	1.001
	24	3	143.1	3.0	429.3	255.1	43.7	1325	1150	1415.427	1.068	1.231
	25	4	101.3	5.0	303.9	347.3	48.1	1177	1310	1330.140	1.130	1.015
	26	5	103.6	4.9	310.8	347.3	48.1	1207	1340	1337.379	1.108	0.998
	27	6	102.0	5.0	306.0	347.3	48.1	1189	1370	1337.990	1.125	0.977
	28	7	142.0	5.1	426.0	347.3	48.1	1969	2160	2172.395	1.103	1.006
	29	8	142.0	5.1	426.0	347.3	48.1	1963	2250	2172.395	1.107	0.966
	30	9	141.4	5.1	424.2	347.3	48.1	1949	2280	2164.551	1.111	0.949
	31	10	141.5	3.1	424.5	255.1	60.8	1621	1920	1879.548	1.159	0.979
	32	11	142.4	3.1	427.2	255.1	60.8	1635	2060	1890.009	1.156	0.917
	33	12	141.6	3.0	424.8	255.1	60.8	1618	1960	1870.496	1.156	0.954
	34	13	103.5	5.0	310.5	347.3	60.8	1331	1500	1526.527	1.147	1.018
	35	14	102.1	5.0	306.3	347.3	60.8	1299	1330	1398.967	1.077	1.052
	36	15	101.9	5.0	305.7	347.3	60.8	1303	1440	1488.587	1.142	1.034
	37	16	142.3	5.1	426.9	347.3	60.8	2193	2520	2433.621	1.110	0.966
	38	17	142.4	5.1	427.2	347.3	60.8	2197	2610	2432.327	1.107	0.932

From the Table 1 and 2 the average of ratio N_O/N_{CAL} and N_O/N_{EXP}, for hollow circular CFST columns is 0.985 and 0.931 with variance of 0.031 and 0.025 respectively, while for solid circular CFST columns it is 0.997 and 1.047 with variance of 0.008 and 0.015 respectively as graphically represent in Fig. 2. For CFST columns with octagonal cross-sectional area from Table 3 and 4 the average of ratio N_O/N_{CAL} and N_O/N_{EXP} is 0.953 and 0.937 with variance of 0.001 and 0.006 respectively for hollow section while for solid section average of ratio N_O/N_{CAL} and N_O/N_{EXP} is 1.168 and 1.089 with variance of 0.004 and 0.013 respectively. A graphical representation of average of ratio N_O/N_{CAL} and N_O/N_{EXP} of octagonal columns is shown in Fig. 2. In the last, from the Table 5 and 6 the average of ratio N_O/N_{CAL} and N_O/N_{EXP}, for hollow square CFST columns is 1.067 and 1.137 with variance of 0.001 and 0.016 respectively, while for solid square CFST columns it is 1.059 and 0.993 with variance of 0.004 and 0.004 respectively, again all the average of ratio N_O/N_{CAL} and N_O/N_{EXP} for square column is shown in Fig. 2. After the comparison, it is cleared that in all cases the analytically and experimentally obtained axial strength is approximately equal to the numerically obtained (using FE models) axial load bearing capacity. The variance is very less for all type of CFST columns with different cross-sectional profiles which indicate that individual N_O/N_{CAL} and N_O/N_{EXP} of every CFST columns does not vary greatly from their mean values. After comparison the interpretation of the obtained result is discussed in the next section of the paper.

5. Result and Discussion

In this section of the manuscript, axial strength obtained from the comparison of load carrying capacity of different CFST columns with up to its failure mechanism to the elastic limit capacity has been discussed as follows.

5.1 Comparison of axial strength of CFST columns

From Fig. 2 (a), numerically obtained axial strength is close to the analytically predicted (based on unified formula) than the axial strength obtained through experiments because $N_O/N_{CAL} > N_O/N_{EXP}$ for of hollow circular CFST columns. It can also be concluded that although the predicted numerical load carrying capacity could be greater or smaller than the experimental test values. But due to average of $N_O/N_{EXP} < 1$, it would be concerned for using numerically modelled axial strength. As it expected to be underestimated. For solid circular CFST column after the comparison as per Fig. 2 (b), the average ratio N_O/N_{CAL} is closer to 1 (1- (N_O/N_{CAL}) =0.003) than the average ratio N_O/N_{EXP} (N_O/N_{EXP})-1=0.047). So, it can be concluded that based on FE models numerically obtained axial strength is closer to the analytically predicted axial strength based on formula. As it could be seen that N_O/N_{EXP} >1 so it may be the numerically predicted Axial strength greater or smaller than experimentally investigated. The probability of axial strength is tending to be overestimated.

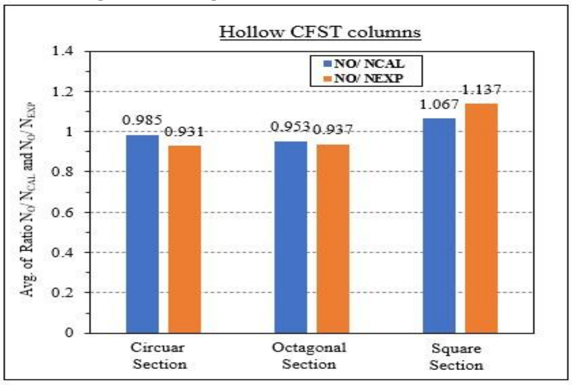

Fig. 2 (a) The average of ratio N_O/N_{CAL} and N_O/N_{EXP} for hollow CFST columns of different cross-sectional areas.

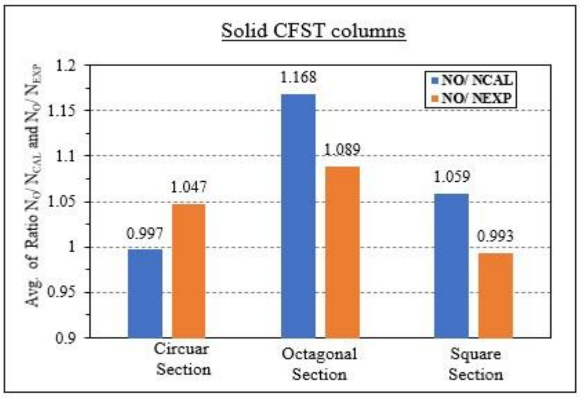

Fig. 2 (b) the average of ratio N_O/N_{CAL} and N_O/N_{EXP} for hollow CFST columns of different cross-sectional area

From Fig. 2 (a) and (b), it is found that for hollow octagonal CFST columns the average ratio of N_0/ N_{CAL} and N_0/ N_{EXP} is less than one. In comparison to the solid octagonal which have N_0/ N_{CAL} and N_0/ N_{EXP} is greater than 1. So, from here it can be concluded that although the numerically obtained axial strength of CFST column having octagonal section profile may be greater or smaller than its experimentally obtained axial strength. Nevertheless, for hollow octagonal CFST columns weather the axial strength is determined by numerically or analytically using mentioned formula the chance of axial strength is to be underestimated. While for solid octagonal CFST it will be expected to be overestimated. One more thing can be concluded that in case of hollow octagonal CFST N_0/ N_{CAL} is closer to 1 than in case of solid octagonal CFST columns which depicts that numerically obtained value of hollow CFST columns is likely to be nearer to the analytically calculated axial strength values in comparison to the solid octagonal CFST columns.

In last for hollow and solid square CFST columns from Fig. 2 (a) and (b) the average ratio of N_0/ N_{CAL} and N_0/ N_{EXP} is either nearly equal to 1 or greater than 1. From this it could be concluded that in both the cases of hollow and solid CFST columns may be the numerically obtained axial load capacity is greater or smaller than the experimentally and analytically obtained axial load capacity. But the chance of numerical obtained axial strength as per FE models is more likely to be overestimated. From average values of N_0/N_{CAL} and N_0/N_{CAL} of both hollow and solid it could be observed that numerically obtained axial strength is almost same as the analytically obtained axial bearing capacity because average of N_0/N_{CAL} is approximately same and nearly equal to 1.

5.2 Failure and Load vs Displacement Curves

All the CFST columns used in Table 1,2,3,4,5 and 6 are geometrically and materially different. So, it is obligatory to select one column from each table which can almost resemble the properties of its remaining columns. In contemplation of those 6 columns were recognized namely, YL-1, 1C-1 and 6D-1 from hollow CFST columns of Table 1, 3 and 5 respectively and SC-4, 3HN, and S1 from solid CFST columns of Table 2, 4 and 6 respectively.

A graphical representation of three different hollow CFST columns, mentioned earlier is shown below in Fig. 3 and a graphical representation of three different solid CFST columns is shown in Fig. 4. From the graphs it could be observed that in case of hollow or solid section initially the relation between the load-displacement curve is linear up to the elastic limit. This initial linear portion indicates that as the load increases the displacement in downward direction along Y-axis is also increased proportionally.

Finite Element models of all 6 columns are presented below with their undeformed and deformed shape in Fig. 5. It can see that as its go down to the column along Y-axis, displacement due to applied load decreases continuously and the upper most portion of all CFST columns have more displacement in comparison to the bottom portion from so it is concluded that displacement is not uniform throughout the CFST columns. Further for the comparison of Experimental, Numerical and Simulated results graph has been plotted among them for the same group of columns from Fig. 6 to 11. These graphs also show the reliability of the adopted. numerical method

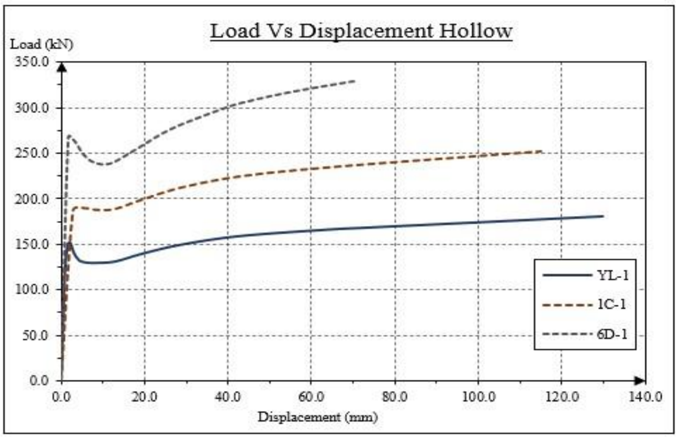

Fig. 3 Load-Displacement curves of Three Different Hollow CFST Columns

Fig. 4. Load-Displacement curve of Three Different Solid CFST Columns

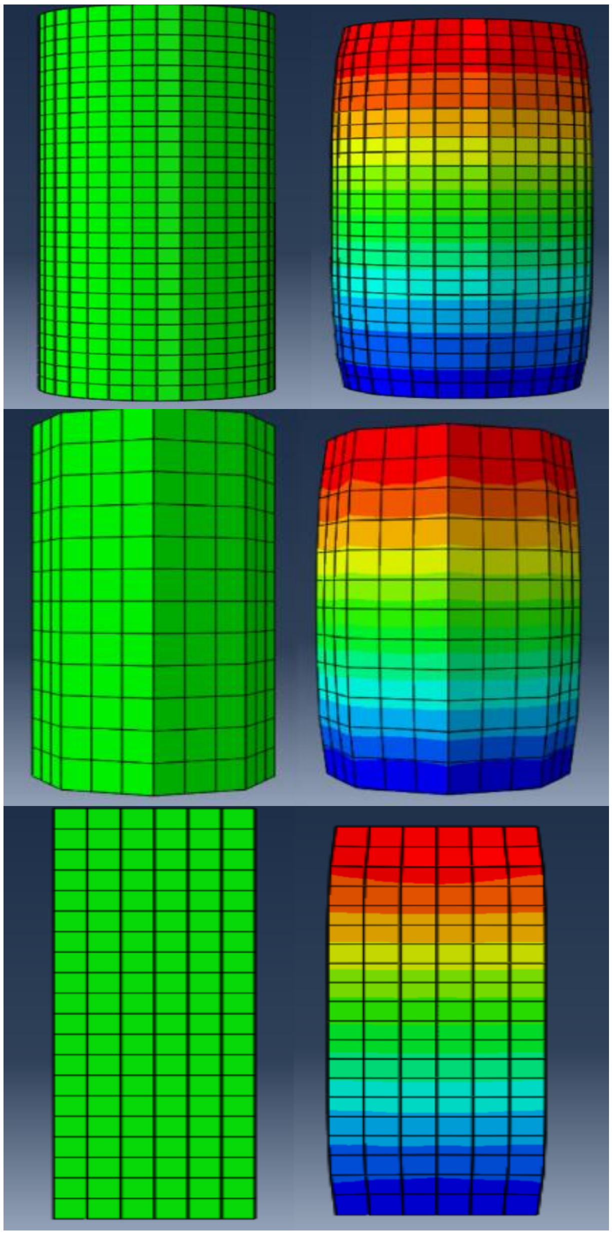

Fig. 5. Deformed and Undeformed CFST Columns

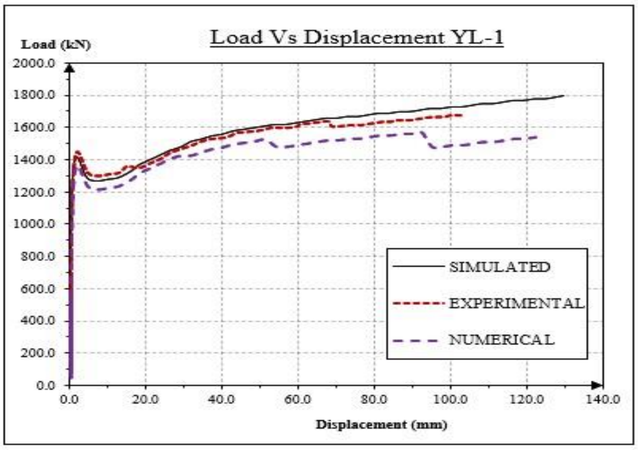

Fig. 6. Load Vs Displacement YL-1

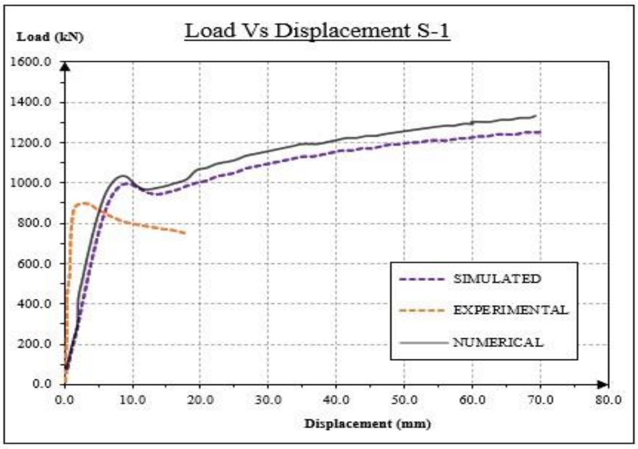

Fig. 7. Load Vs Displacement S-1

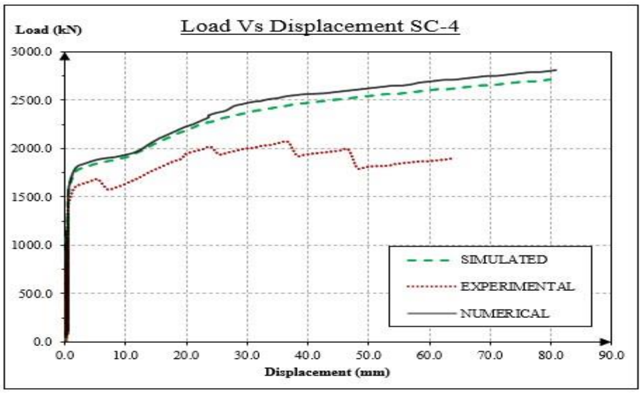

Fig. 8. Load Vs Displacement SC-4

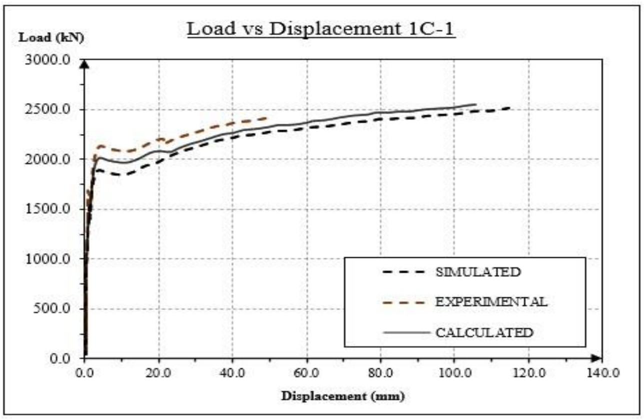

Fig. 9. Load Vs Displacement 1C-1

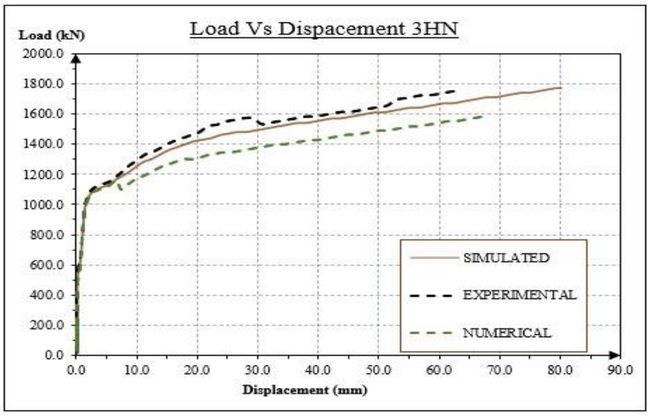

Fig. 10. Load Vs Displacement 3HN

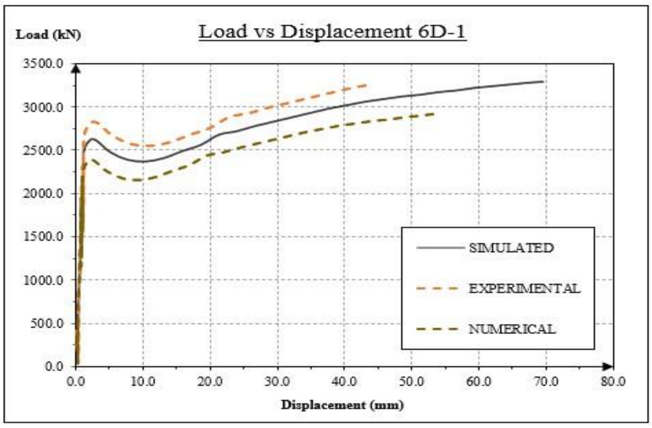

Fig. 11. Load Vs Displacement 6D-1

6. Conclusions

The unified formula put forwarded by Yu M. et al. (2010) for envisaging the axial load carrying capacity of CFST columns irrespective to the sectional profile of columns. This formula is verified by the numerical methods using Finite Element models and test data results. Following inference have been determined:

1. The proposed unified formula predicts a satisfactory outcome once compared with the outcome of Finite Element models which has been shown in the load displacement curves.

2. Although the axial compressive strength of CFST columns obtained numerically based on Finite Element models may be greater or smaller individually, it most likely to underestimate the hollow circular and octagonal section.

3. As the load increases initially the relation between load and displacement is linear but as load kept on continuously increasing then after some time (when concrete got crushed) then variation between load and displacement will be no longer linear.

4. The sudden change in the curve of load displacement relation of hollow CFST column is more in comparison to the solid CFST column because of available space in hollow CFST provided space to concrete got crushed with in the tube itself.

5. On increased load, displacement in CFST columns does not take place equally throughout the columns along its length. Instead, most of the displacement occurs in the topmost portion of the columns.

6. Displacement is mainly in the upper portion of CFST column just below the place of application of load.

Lastly, it can be concluded that the unified formula obtained from mentioned formulas have good agreement with Finite Element models and have potential to use in industry.

7. Future Scope

Future work is required to extend the formulas of load carrying capacity of CFST columns to incorporate the effect of temperature elevation. It is also required more verification of this unified formula for octagonal hollow and solid sections because very few literatures are available on this which could show the behavior of hollow and solid CFST columns. Further research is needed to extend the proposed formula to other types of loading, such as bending and shear. Ring confinement technique or any other technique can be used to protect the zone of maximum compression so that axial strength also gets increased.

References

ABAQUS (2013), Standard user's manual, version 6.13, Dassault Systems Corp.

ACI 318-08. (2008). Building Code Requirements for Structural Concrete. Farmington Hills, MI: American Concrete Institute.

Architectural Institute of Japan, AIJ, (2008). Recommendations for Design and Construction of Concrete Filled Steel Tubular Structures. Tokyo, Japan.

AISC LRFD. (2000). Load and Resistance Factor Design Specification for Structural Steel Buildings. Chicago, IL: American Institute of Steel Construction.

BS5400-5 (2005). "Steel, concrete and composite bridge's part 5" code of practice for the design of composite bridges, London (UK).

Chinese Code, D. L. T. (1999). Chinese design code for steel-concrete composite structures. DL/T 5085-1999.

CEN, European Committee for Standardization: (2002). "Eurocode—Basis of structural design" EN 1990. Brussels, Belgium: CEN.

CEN, European Committee for Standardization: (2005). "Eurocode3: Design of steel structures—Part 1-1: General rules and rules for buildings" EN 1993-1-1. Brussels, Belgium: CEN.

Dai, X. H., Lam, D., Jamaluddin, N., & Ye, J. (2014). "Numerical analysis of slender elliptical concrete filled columns under axial compression." Thin-Walled Structures, 77, pp. 26-35.

Dey, P., Gupta, R. K., & Laskar, A. I. (2019). "Numerical and experimental investigations of different cross-sectional configuration of plain concrete and CFST short columns under axial compression." International Journal of Civil Engineering, 17(10), pp. 1585-1601.

Evirgen, B., Tuncan, A., & Taskin, K. (2014). "Structural behavior of concrete filled steel tubular sections (CFT/CFSt) under axial compression." Thin-Walled Structures, 80, pp. 46-56.

Fam, A., Qie, F. S., & Rizkalla, S. (2004). "Concrete-filled steel tubes subjected to axial compression and lateral cyclic loads." Journal of Structural Engineering, 130 (4), pp. 631-640.

Giakoumelis, G., & Lam, D. (2004). "Axial capacity of circular concrete-filled tube columns." Journal of Constructional Steel Research, 60(7), pp. 1049-1068.

Gupta, P. K., Sarda, S. M., & Kumar, M. S. (2007). "Experimental and computational study of concrete filled steel tubular columns under axial loads." Journal of Constructional Steel Research, 63(2), pp. 182-193.

Gupta, P. K., Ahuja, A. K., & Khaudhair, Z. A. (2014). "Modelling, verification and investigation of behaviour of circular CFST columns." Structural Concrete, 15(3), pp. 340-349.

Gupta, P. K., & Singh, H. (2014). "Numerical study of confinement in short concrete filled steel tube columns." Latin American Journal of Solids and Structures, 11, pp. 1445-1462.

Hafezolghorani, M., Hejazi, F., Vaghei, R., Jaafar, M. S. B., & Karimzade, K. (2017). "Simplified damage plasticity model for concrete." Structural Engineering International, 27(1), pp. 68-78.

Han, L. H. (1997). "Theoretical analysis and experimental research for the behaviors high strength concrete-filled steel tubes." Industrial Construction, 27 (11), pp. 39 - 44.

Han, L. H. (2000). "Tests on concrete filled steel tubular columns with high slenderness ratio." Advances in Structural Engineering, 3(4), pp. 337-344.

Han, L. H., Wang, W. D., & Tao, Z. (2011). "Performance of circular CFST column to steel beam frames under lateral cyclic loading." Journal of Constructional Steel Research, 67(5), pp. 876-890.

He, L., Zhao, Y., & Lin, S. (2018)., "Experimental study on axially compressed circular CFST columns with improved confinement effect." Journal of Constructional Steel Research, 140, pp. 74-81.

Lai, M. H., & Ho, J. C. M. (2014). "Confinement effect of ring-confined concrete-filled-steel-tube columns under uniaxial load." Engineering Structures, 67, pp. 123-141.

Lee, S. H., Uy, B., Kim, S. H., Choi, Y. H., & Choi, S. M. (2011). "Behavior of high-strength circular concrete-filled steel tubular (CFST) column under eccentric loading." Journal of Constructional Steel Research, 67(1), pp. 1-13.

Li B., & Hao, R. X. (2005). "The analysis of concrete filled steel tube column carrying capacity." Journal of Baotou University Iron Steel Technology, 24(1), pp. 5-8.

Liew, J. R. (2015). "Design guide for concrete filled tubular members with high strength materials to Eurocode 4." Research publishing.

Liu, D., & Gho, W. M. (2005). "Axial load behaviour of high-strength rectangular concrete-filled steel tubular stub columns." Thin-Walled Structures, 43(8), pp. 1131-1142.

Liu, D. (2005). "Tests on high-strength rectangular concrete-filled steel hollow section stub columns." Journal of Constructional Steel Research, 61(7), pp. 902 - 911.

Shakir-Khalil, H. (1993). "Pushout strength of concrete-filled steel hollow section tubes." Structural Engineer, 71(13).

Shakir-Khalil, H. (1993). "Resistance of concrete-filled steel tubes to pushout forces." Structural Engineer, 71(13).

Shanmugam, N. E. and Lakshmi, B., (2001) "State of the art report on steel–concrete composite columns", Journal of constructional steel research, 57 (10) , pp 1041-1080.

Singh, V. K., P. K. Gupta and S. M. Ali Jawaid (2022) "Bond strength characterization of concrete filled steel tube as structural member", Electronic Journal of Structural Engineering, 22(2), pp. 42–52.

Schneider, S. P. (1998). Axially loaded concrete-filled steel tubes. Journal of structural Engineering, 124(10), 1125-1138.

Tao, Z., Han, L. H., Uy, B., & Chen, X. (2011) "post-fire bond between the steel tube and concrete in concrete-filled steel tubular columns." Journal of Constructional Steel Research, 67(3), pp. 484-496.

Tao, Z., Wang, Z. B., & Yu, Q. (2013) "Finite element modelling of concrete-filled steel stub columns under axial compression." Journal of constructional steel research, 89, pp.-121-131.

Tao, Z., Song, T. Y., Uy, B., & Han, L. H. (2016) "Bond behavior in concrete-filled steel tubes." Journal of Constructional Steel Research, 120, pp. 81-93.

Thai, H. T., Uy, B., Khan, M., Tao, Z., & Mashiri, F. (2014) "Numerical modelling of concrete-filled steel box columns incorporating high strength materials." Journal of Constructional Steel Research, 102, pp. 256-265.

Xiong, M. X., Xiong, D. X., and Liew, J. R. (2017) "Axial performance of short concrete filled steel tubes with high-and ultra-high-strength materials." Engineering Structures 136, pp. 494-510.

Yadav, R., Chen, B., Huihui, Y., & Lian, Z. (2016, October). "Numerical study on the seismic behavior of CFST columns." In 11th Pacific Structural Steel Conference, Shanghai, China, October (Vol. 2931, pp. 360-369).

Yang, Y. F., & Han, L. H. (2011). "Behaviour of concrete filled steel tubular (CFST) stub columns under eccentric partial compression." Thin-Walled Structures, 49(2), pp. 379-395.

Yu, M., Zha, X., Ye, J., & She, C. (2010). "A unified formulation for hollow and solid concrete-filled steel tube columns under axial compression." Engineering structures, 32(4), pp. 1046-1053.

Yu, M., Zha, X., Ye, J., & Li, Y. (2013). "A unified formulation for circle and polygon concrete-filled steel tube columns under axial compression." Engineering structures, 49, pp. 1-10.

Yu, Q., Tao, Z., & Wu, Y. X. (2008). "Experimental behaviour of high-performance concrete-filled steel tubular columns." Thin-Walled Structures, 46(4), pp. 362-370.

Zha X. (2010). "Hollow and solid concrete-filled steel tube structures" Beijing: Science Press, 2010.

Zhang, W., & Shahrooz, B. M. (1999). "Comparison between ACI and AISC for concrete-filled tubular columns." Journal of structural engineering, 125(11), pp. 1213-1223.

Zhong, S. T. (2006). "Research and application achievement of concrete-filled steel tubular (CFST) structures." Beijing: Tsinghua University Press, China.

Zhong S. T. (2003) "Concrete-filled steel tubular (CFST) structures." Beijing: Tsinghua University Press.

Zhang, S., Guo, L., Ye, Z., & Wang, Y. (2005). "Behavior of steel tube and confined high strength concrete for concrete filled RHS tubes." Advances in Structural Engineering, 8(2), pp. 101-116.